$d\sigma/dy$ distribution of Drell-Yan dielectron pairs

Jiyeon Han, A. Bodek, W. Sakumoto, Y. Chung

University of Rochester, NU 14627-0171 USA

E-mail: jyhan@fnal.gov

Abstract. We report on the measurement of the rapidity distribution, $d\sigma/dy$, over the full kinematic range for e^+e^- pairs produced in $p\bar{p}$ collisions at $\sqrt{s} = 1.96$ TeV in the Z boson region of $66 < M_{ee} < 116$ GeV/c^2. The data sample consists of 1.1 fb^{-1} of $p\bar{p}$ collisions at $\sqrt{s} = 1.96$ TeV taken by the Collider Detector at Fermilab (CDF). The $d\sigma/dy$ is compared with the NLO theory prediction.

1. Introduction

Measurement of the rapidity distribution and total cross section of e^+e^- pairs from γ^*/Z production provide a stringent test of QCD calculations in leading order (LO) and next to leading order (NLO). Figure 1 shows the Feynman diagram for γ^*/Z boson production in the $p\bar{p}$ collision. In leading order, the process is $q + \bar{q} \rightarrow \gamma^*/Z$, i.e. a quark and anti-quark from the colliding hadrons annihilates to form a virtual γ^*/Z boson. Two partons, carrying momentum fractions x_1 and x_2, participate in the interaction. The final state from this process is a pair of leptons from the γ^*/Z decay. The emission of gluons in the initial state is taken into account in calculations which include corrections beyond the leading order in the strong interaction. In LO, the momentum fraction $x_1(x_2)$ carried by the partons from the proton(antiproton) is related to the rapidity (y) of the Z boson via the equation:

$$x_1 = M_Z e^y s^{-1/2} \ , \ x_2 = M_Z e^{-y} s^{-1/2} \tag{1}$$

where s is the center of mass energy and M_z is the dielectron invariant mass. Figure 2 shows $x_1(x_2)$ as a function of y at the Tevatron, $\sqrt{s} = 1.96$ TeV.

In this analysis, the $d\sigma(\gamma^*/Z)/dy$ distribution is measured using dielectrons from γ^*/Z decays. This analysis includes e^+e^- pairs from the forward calorimeter region.

2. Event Selection

The data sample consists of $1.1 fb^{-1}$ taken with the CDF Run II Detector. The events are selected from the inclusive single high pt electron in the central calorimeter or two high pt electrons in both central or forward calorimeter trigger data sets. The electron trigger efficiencies as a function of E_T are measured using the data. The individual electron trigger efficiencies are combined to form the overall trigger efficiency of electron pairs versus its rapidity. The overall trigger efficiencies are almost 100%. The dielectron data sample consists of three different e^+e^- pair topologies: The CC, CP, and PP topologies. The CC topology has two electrons in the central calorimeter with $|\eta| < 1.1$ and the electrons have the opposite electric charge. The CP topology has one electron in the central calorimeter with $|\eta| < 1.1$, and another in the plug

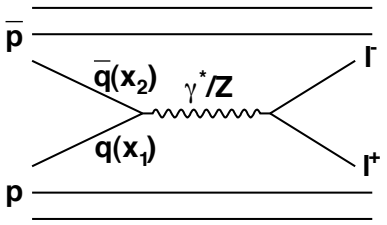

Figure 1. Feynman diagram of LO γ^*/Z production in a $p\bar{p}$ collision.

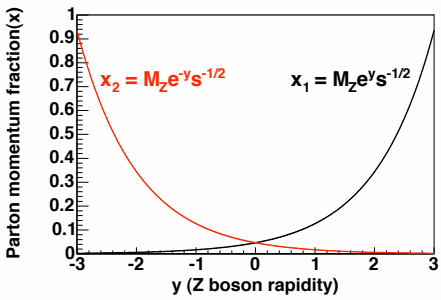

Figure 2. The relationship between the momentum fraction, x, and the rapidity of the γ^*/Z boson.

calorimeter with $1.2 < |\eta| < 2.8$. The PP topology has two electrons in the plug calorimeter with $1.2 < |\eta| < 2.8$ and with both electrons on the same calorimeter side. All electrons used in the analysis are high pt electrons($E_T \geq 25$ GeV for CC and PP, $E_T \geq 20$ GeV for CP) and required to pass electron identification cuts. The PP topology has more background than other topologies, so at least one electron must have a matching silicon track to reduce the background. The overall silicon tracking efficiency is 87%. After selection cuts, we find 28097 CC topology events, 46676 CP topology events, and 16589 PP topology events (total = 91362 events). The rapidity of events reaches $|y| = 2.9$ with the addition of PP topology events.

3. Acceptance and Efficiencies

Geometric and kinematic acceptances are modeled by using the *Pythia*[1] $Z \rightarrow ee$ event generator combined with a *GEANT*[2] simulation of the CDF detector. The simulation is tuned to data for the energy resolution and efficiencies (electron ID and silicon tracking efficiency). The acceptance(A) and efficiencies(ϵ) are measured as a function of the boson rapidity. Figure 3 shows the $A \times \epsilon$ as a function of the γ^*/Z boson rapidity. The $A \times \epsilon$ is flat up to $y \sim 2.0$ and is non-zero up to $|y| = 2.9$ with the PP topology.

4. Background Estimation

The main source of background in the analysis is QCD dijet background, which is measured separately in each dielectron topology using data. The background from electroweak(WW, WZ, and W inclusive) and $t\bar{t}$($t\bar{t}$ inclusive) processes are also considered and the background rates and shapes for these processes are measured using simulation.
The total backgrounds are summarized in Table 1.

Table 1. The background rates and total systematic uncertainties.

Topology	Background Rate (unit: %)
CC	$0.38 \pm 0.08(stat.) \pm 0.11(sys.)$
CP	$0.65 \pm 0.08(stat.) \pm 0.20(sys.)$
PP	$2.62 \pm 0.22(stat.) \pm 0.79(sys.)$

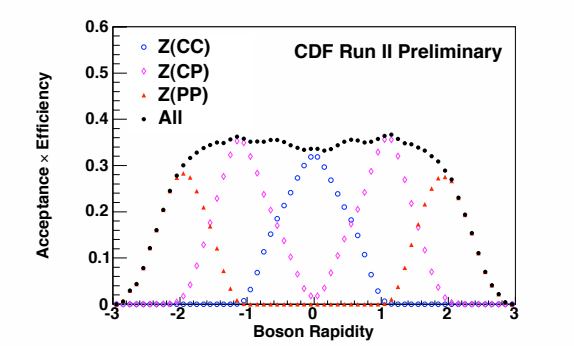

Figure 3. The product of the kinematic acceptance and the event selection efficiencies versus the dielectron rapidity.

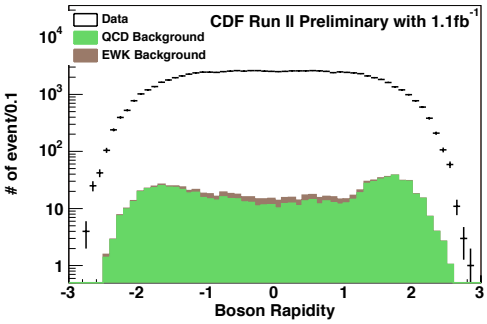

Figure 4. The dielectron rapidity distribution of the data and the backgrounds.

5. Systematic Uncertainties

Systematic uncertainties are determined for;

- Detector material modelling ($\delta\sigma/\sigma = 0.1\%$)
- Background estimates (0.4%)
- Electron identification efficiencies (1.3%)
- Silicon tracking efficiency (0.2%)
- Acceptance (0.1%)

The largest systematic uncertainty is associated with the measurement of the electron identification efficiencies.

6. $d\sigma/dy$ Measurement

Figure 4 shows the dielectron rapidity distributions of the data after all selection cuts. We measure the $d\sigma/dy$ distribution of the dielectron pairs using:

$$\frac{d\sigma(\gamma^*/Z)}{dy}(y) = \frac{N_{sig}(y) - N_{bkg}(y)}{\Sigma_i A_i \times \epsilon_i(y) \cdot \epsilon^i_{trig}(y) \cdot \epsilon_{zvtx} \cdot \int Ldt} \tag{2}$$

where $N_{sig}(y) - N_{bkg}(y)$ is the number of the background-subtracted events, the sum i is over the dielectron topologies(CC, CP, PP) $A_i \times \epsilon_i(y)$ is the combined acceptance and efficiency (Figure 3), and the $\epsilon^i_{trig}(y)$ is the trigger efficiency of each topology, the $\epsilon_{zvtx} = 95.5 \pm 0.4\%$ is the acceptance for the $p\bar{p}$ collision vertex to occur in the central 60 cm of the detector, and $\int Ldt$ is the total integrated luminosity.

The $d\sigma(\gamma^*/Z)/dy$ measurement is shown in Figure 5 separately for the positive and negative rapidity. The total cross section from integrating $d\sigma(\gamma^*/Z)/dy$ is $\sigma = 263.34 \pm 0.93(statistic) \pm 3.79(systematic)$ pb. The luminosity error of 6% is not included in the systematic error of the total cross section measurement. Since the measured $d\sigma/dy$ is symmetric about y=0, we combine the results and this is shown in Figure 6.

We compare the data to three different theory predictions. The perturbative calculation is an NLO and NNLO QCD calculation. Two different PDFs are used: CTEQ6 and MRST2001E [4, 5]. The total predicted cross section is normalized to the measured cross section, 263.34 pb. Figure 7 and 8 show the data to theory ratios. It shows a good agreement between data and predictions and is more consistent with NLO calculation with NLO CTEQ6 PDF.

7. Conclusion

CDF collaboration has measured the $d\sigma/dy$ differential cross section for $p\bar{p} \to Z^0/\gamma^* \to e^+e^-$. The total cross section integrated over all dielectron rapidities is $\sigma = 263.34 \pm 0.93(statistic) \pm 3.79(systematic)$ pb. The main goal of the analysis is to compare the shape between data and theory predictions and future input to PDF fits. We find the NLO calculation with NLO CTEQ6.1 PDF to be more consistent with the data.

References

[1] Torbjrn Sjstrand et al JHEP05(2006)026, hep-ph/0603175.
[2] http://wwwasd.web.cern.ch/wwwasd/geant/
[3] CDF collaboration: T.Affolder, et al. Phys.Rev. D63(2001), hep-ex/0006025.
[4] A.D. Martin, R.G. Roberts, W.J. Stirling, and R.S. Thorne, Eur.Phys.J. C28(2003), hep-ph/0211080.
[5] J. Pumplin, D.R. Stump, J. Huston, H.L. Lal, P.Nadolsy, W.K. Tung, JHEP 0207(2002) 012, hep-ph/0201195.

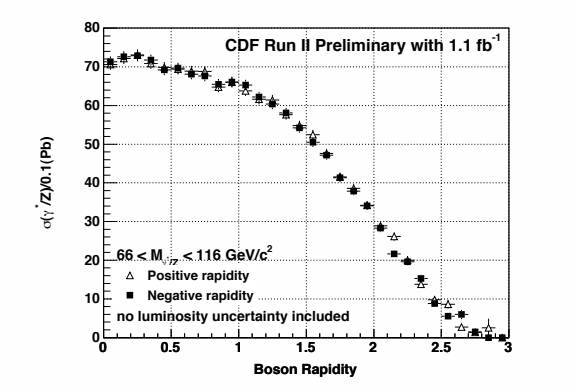

Figure 5. The measured $d\sigma/dy$ for $p\bar{p} \to Z^0/\gamma^* \to e^+e^-$ in the negative and positive rapidity.
Only statistic uncertainties are considered.

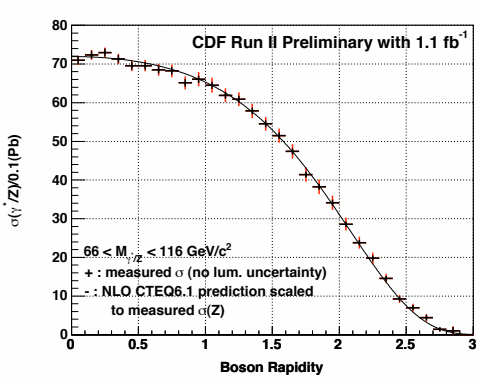

Figure 6. The measured $d\sigma/dy$ for $p\bar{p} \to Z^0/\gamma^* \to e^+e^-$. The crosses are the measurement and the solid line is the theory prediction. The prediction is the NLO calculation with NLO CTEQ6.1

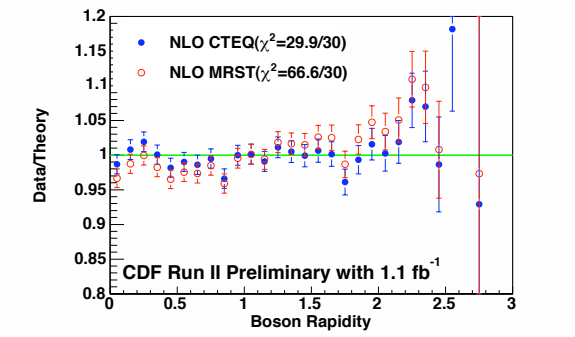

Figure 7. The ratio of the data to the theory prediction for $d\sigma/dy$.
For theory predictions, CTEQ6 and MRST2001E PDF sets with NLO calculation are used.

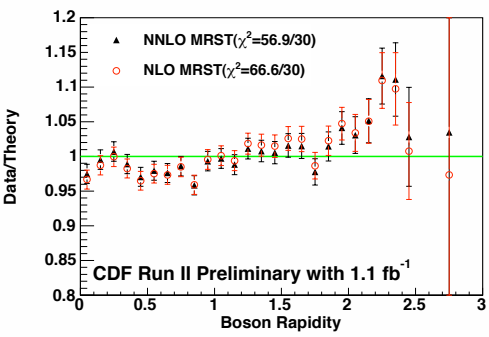

Figure 8. The ratio of the data to the theory prediction for $d\sigma/dy$.
For theory predictions, NNLO and NLO calculations with MRST PDF set are used.